nature photonics

LETTERS

PUBLISHED ONLINE: 23 JANUARY 2011 | DOI: 10.1038/NPHOTON.2010.314

High-resolution broad-bandwidth Fourier-transform absorption spectroscopy in the VUV range down to 40 nm

Nelson de Oliveira[1]*, Mourad Roudjane[1†], Denis Joyeux[1,2], Daniel Phalippou[2], Jean-Claude Rodier[2] and Laurent Nahon[1]

Vacuum-ultraviolet (VUV) high-resolution absorption spectroscopy is a unique tool for the study of gas-phase atomic and molecular electronic structure. To date, it has been performed by using lasers or synchrotron radiation-based grating spectrometers, but none of these techniques can offer simultaneous high resolution, wavelength accuracy and broad tunability. The only technique combining these three important features is Fourier-transform spectroscopy, but this is limited to the mid-UV range (down to 140 nm; ref. 1) because of a lack of beamsplitters. Here, we present a new instrument based on a wavefront-division scanning interferometer, applied for the first time to the VUV range. This instrument, coupled to the DESIRS beamline at synchrotron SOLEIL, covers a broad range of wavelengths (typically 7%, adjustable in the 250–40 nm range), a resolving power of $\sim 1 \times 10^6$, an extrinsic absolute wavelength accuracy of 1×10^{-7} and a high signal-to-noise ratio.

In the VUV range, the currently available optical spectroscopic techniques use either gratings or lasers. Lasers are naturally targeted at narrow spectral range experiments associated with ultrahigh resolution. Recent improvements regarding tunable VUV laser sources give access to unprecedented resolving power ($\sigma/\delta\sigma > 1 \times 10^7$) and wavenumber accuracy ($\Delta\sigma/\sigma$ as low as 6×10^{-9}) with a limited tunability[2–6]. In contrast, grating-based spectroscopy from a broadband continuum allows a large spectral domain covering, but suffers from resolution limitations due to the optical quality that can be achieved on gratings of large size and with high groove densities. In particular, the resolving power of grating-based spectrometers can barely reach 100,000–200,000, depending on the VUV region[7–9]. On the other hand, from the far-infrared to the near-VUV range (~140 nm), Fourier-transform spectroscopy has been an important spectroscopic tool because of its unique combination of properties: a very high resolving power and accurate absolute spectral data over a large spectral range, associated with a multiplex-wavelength acquisition scheme.

In this Letter, we demonstrate for the first time the extension of high-resolution Fourier-transform spectroscopy into the windowless VUV range down to 40 nm. Fourier-transform spectroscopy is usually based upon amplitude division through beamsplitters, as exemplified in the Michelson interferometer geometry. However, the manufacture of beamsplitters is difficult and even impossible in the far-VUV range ($\lambda < 140$ nm). This is the main reason why amplitude-division Fourier-transform spectroscopy has never been extended to higher energies[1,10]. In this situation, wavefront-division interferometers offer an alternative approach. For example, a lamellar grating interferometer has already been operated in the far-infrared region[11]. Another solution was specifically designed for the study of autoionization processes in doubly-excited helium around $\lambda = 19$ nm, but, as far as we know, it was never successful in this aim[12].

To overcome the beamsplitter problem and with a view to achieving a broadband VUV Fourier-transform spectrometer (FTS), we designed a scanning wavefront-division interferometer based on a variation of the Fresnel bimirror interferometer[13]. The overall geometry of the actual instrument is depicted in Fig. 1. This is quite similar to the geometry of our first prototype[14], with which we were able to record the Schuman–Runge bands of O_2 around 190 nm at the limit transmission of ambient air with a resolving power of 150,000. Although the basic principles are the same, the present instrument was fully rebuilt and upgraded to cover the 250–40 nm (5–30 eV) range and to be compatible with ultrahigh-vacuum (UHV) conditions. It is now a permanent end-station on the VUV beamline DESIRS[15] of the SOLEIL synchrotron facility in France, where the undulator[16] provides an ideal, coherent, 7% bandwidth continuum background.

The upgraded scanning control system is based on a multireflection HeNe laser interferometer arrangement, which produces the sampling comb with the required sampling interval for broad spectral range recording (Fig. 1b). Its mobile mirror is the backside of the VUV mobile reflector, and guarantees a direct and stable relation between the VUV optical path difference (OPD) changes and the visible interferometric control signal. A VUV silicon photodiode records the interferogram on the fly. The visible interferogram has a period $\delta x = \lambda_{HeNe}/2p'$ in terms of reflector displacement, where p' equals the number of reflections p of the multireflection system, multiplied by a geometrical factor that is p-dependent and close to one[14]. This interferogram is used to trigger VUV interferogram sampling twice per period, that is, each $\lambda_{HeNe}/4p'$ in terms of displacement or $\lambda_{HeNe}/2p'$ in terms of the VUV OPD, as a result of the system geometry. This leads to a p-dependent free spectral range $\Delta\sigma = 1/2\delta x = p'\sigma_{HeNe}$. In the new updated instrument, p is an adjustable parameter in the range 8–15, allowing adaptation of the free spectral range to the spectral region to be covered. This adjustment is carried out by tilting the mobile reflector block (Fig. 1). In Fourier-transform spectroscopy, the resolving power depends on the maximum OPD that can be reached, and therefore on the maximal travelling range offered by the scanning system. In this instrument, the multireflection ray path extends laterally in the plane of the diagram by an amount proportional to the OPD, but also roughly proportional to p^2. As this extension cannot be larger than the mirror size, the maximum OPD is in fact limited by p,

[1]Synchrotron Soleil, Orme des Merisiers St Aubin BP 48, 91192 GIF sur Yvette Cedex, France, [2]Laboratoire Charles Fabry de l'Institut d'Optique, RD 128, Campus Polytechnique, 91127 Palaiseau Cedex, France; [†]Present address: Department of Chemistry, 009 Chemistry-Physics Building, University of Kentucky, 505 Rose Street, Lexington, Kentucky 40506-0055, USA. *e-mail: nelson.de.oliveira@synchrotron-soleil.fr

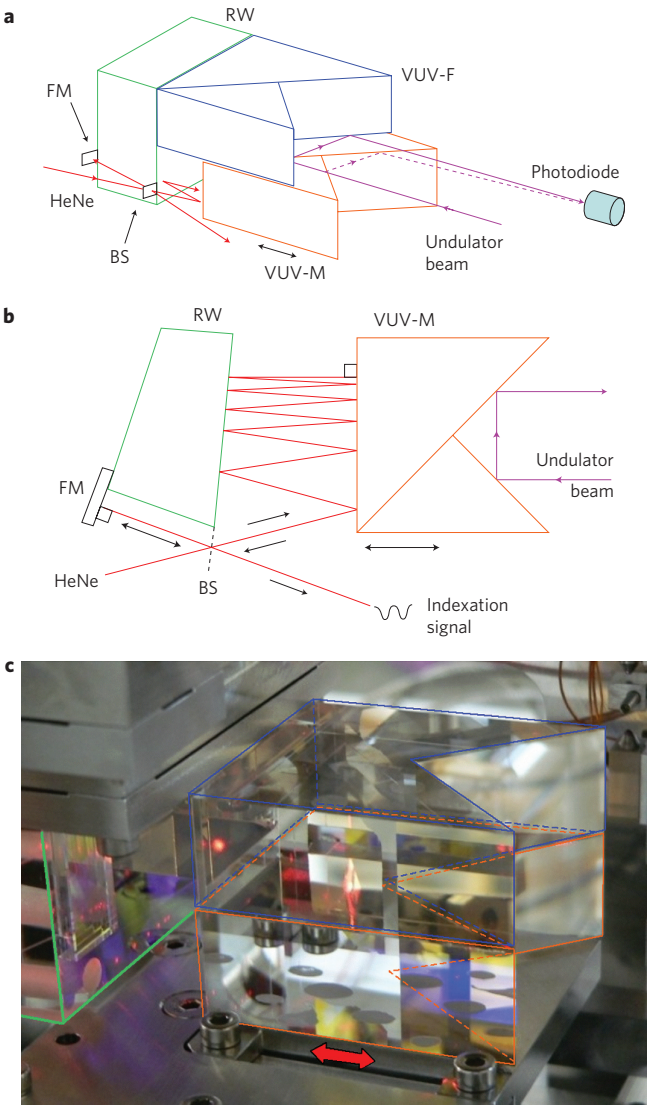

Figure 1 | VUV scanning wavefront-division interferometer. **a**, Two distinct roof-shaped optical blocks consisting of two VUV reflective surfaces meeting at an angle of 90° face the incident VUV undulator beam. The reference reflector (VUV-F) and the mobile reflector (VUV-M) are separated by a 100 μm gap. The VUV beam incident on the adjacent edges is divided and reflected twice at an incidence angle of 45° by the two reflectors. The two reflected beams overlap and interfere downstream due to a small vertical tilt of the top reflector. The interferogram is detected by a VUV photodiode located 130 cm downstream of the reflectors, just behind a horizontal 50 μm slit, smaller than the spatial fringe spacing. Note that wavefront-division interferometers require a certain degree of one-dimensional spatial coherence, which is provided by the DESIRS undulator source. **b**, VUV-M motion is measured using a visible interferometer based on a multireflections scheme between two plane mirrors. (HeNe, HeNe frequency-stabilized laser beam; FM, fixed mirror; BS, beamsplitter of the control interferometer). After the beamsplitter, the beam is reflected p times ($p = 11$ in this case) between the plane surface at the back of the VUV-M and a reference wedge (RW) prism and then returns. **c**, Image of the mounted VUV wavefront-division interferometer. Note the HeNe laser beam spots onto the reference wedge prism plane surface.

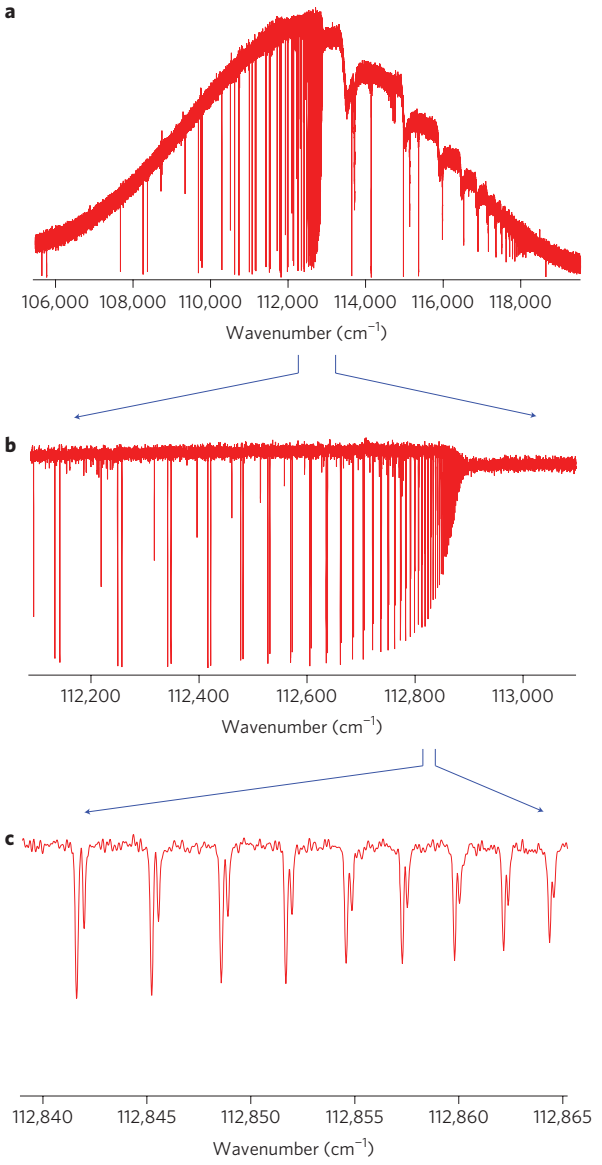

Figure 2 | Krypton absorption spectrum showing the Rydberg series converging towards the $4p^{-1}$ ($^2P_{3/2}$) and ($^2P_{1/2}$) ionization limits. The LN_2-cooled windowless gas cell was used with a pressure of 0.01 mbar. Acquisition time for the spectrum is 4 h (80 scans), with $p = 9$, using the full travelling range allowed by the control system (32.5 mm, corresponding to 1,840,000 independent samples). **a**, Full spectrum showing the 7% bandwidth undulator envelope. **b**,**c**, Close-ups of parts of the spectrum in **a**. Total raw measured linewidth is 0.13 cm^{-1} (resolving power of 850,000), which, after deconvolution of the theoretical instrumental linewidth, yields a Doppler broadening of 0.095 cm^{-1} corresponding to a gas temperature of ~110 K.

the longitudinal allowed travel always being larger. In other words, both the ultimate resolution and the free spectral range are determined by p. This is illustrated in Table 1, where the full-width at half-maximum (FWHM) of the instrumental linewidth $\delta\sigma$ (which is a sinc function as in any unapodized Fourier-transform spectrum) is calculated for each p, considering recording of a typical $1{,}024^2$ independent samples, a condition that can be met for all p. However, a larger scan can be obtained for $8 \leq p \leq 14$, leading to a significant improvement of the resolution, as shown in Table 1. As the scan is essentially single-sided, a phase-correction procedure is required[17]. To this end, the scan is extended beyond the zero OPD position to obtain a short double-sided interferogram.

Instrument resolution has been measured throughout the VUV range for rare gases, used as model systems, by using a gas sample chamber specifically developed for the FTS. This sample chamber includes two different set-ups: a windowless gas cell that can be

Table 1 | Calculated instrument width.

p	8	9	10	11	12	13	14	15
Nyquist frequency (cm^{-1})	125,639	141,344	157,051	172,752	188,456	204,160	219,863	235,566
FWHM $\delta\sigma$ (cm^{-1}) $1{,}024^2$ samples	0.14	0.16	0.18	0.20	0.22	0.23	0.25	0.27
Ultimate FWHM $\delta\sigma$ (cm^{-1})	0.075	0.090	0.11	0.13	0.15	0.18	0.22	0.27

The *p* parameter sets the VUV interferogram sampling interval. First row, free spectral range; second row, absolute instrumental linewidth for $1{,}024^2$ independent samples; third row, absolute instrumental linewidth for the maximum travel allowed by the scanning system (the corresponding number of samples depends on *p*).

cooled with liquid nitrogen (LN_2) and a free expansion jet. We present an example of each set-up. Figure 2 shows the recorded valence-shell photoabsorption spectrum of krypton. The full Rydberg series spectrum converging towards the $4p^{-1}$ ($^2P_{3/2}$) and ($^2P_{1/2}$) ionization limits was recorded in 4 h, setting the instrument to its maximum resolving power at $p = 9$ ($\delta\sigma = 0.09\ cm^{-1}$; see Table 1). To decrease Doppler broadening, the windowless LN_2-cooled gas cell was used. The total raw measured linewidth is $0.13\ cm^{-1}$ and corresponds to a totally unprecedented raw resolving power of 850,000. Once deconvolved from the theoretical instrumental linewidth, this spectrum yields a Doppler width of $0.095\ cm^{-1}$ corresponding to a gas temperature of ~110 K. The spectrum shown in Fig. 2 is the highest resolution spectrum, by a factor of 6, ever published for the complete Rydberg structure of a rare gas[18]. Figure 3 shows the photoabsorption cross-section spectrum of helium seeded in argon and cooled by the adiabatic expansion obtained in the atomic beam. The contribution from the cooled part appears as a sharp line ($0.29\ cm^{-1}$ measured width) on a broad pedestal corresponding to the room-temperature background gas.

A major factor in spectroscopy is the absolute precision of the energy scale. Because some of the angular parameters are not known with the required accuracy, the ultimate intrinsic precision of the FTS apparatus is in the range of 1×10^{-6} to 2×10^{-6} without any external calibration, in other words, about two orders of magnitude better than that for a grating-based spectrometer[7]. To reach a higher level of precision, we used different reference lines from the literature that have been measured precisely by laser spectroscopy. Because of the linearity property of the Fourier transform, the procedure of referencing to a single known spectral line is always easy and direct. This is not the case for grating-based spectroscopic methods, where it is necessary to have a set of references distributed throughout the region of interest. Following this procedure and using two reference laser-based measurement lines[19], internal statistical uncertainty from run to run was checked for the argon case on five different scans. The resulting standard deviation on the measured position of the lines was within 1×10^{-7}, a value that is consistent with the expected line position uncertainties given by the empirical relation[20]

$$\Delta\sigma = \frac{f}{\sqrt{N}}\frac{W}{\mathrm{SNR}}$$

where SNR is the signal-to-noise ratio, W is the linewidth, N is the number of independent points per linewidth, and f is a constant of the order of unity that is lineshape-dependent. Relative intensity branching ratios can be accurately measured with the Fourier-transform spectroscopy technique, with all wavelengths recorded at the same time. This contrasts with the situation in a sequential instrument, in which small drifts in the column density can ruin a measurement covering a large spectral range.

Another important issue to be considered is the signal-to-noise ratio in the spectrum. In absorption Fourier-transform spectroscopy, the signal (that is, the depth induced by the spectral absorption line under the local source level), depends on the spectral feature under consideration through the ratio of the molecular linewidth to the instrumental resolution. Assuming that the interferogram noise is white, the noise in the spectrum varies in proportion to the square root of the number of interferogram samples. In other words, by keeping the OPD sampling interval constant, the spectral noise increases with resolution (this has been checked in experimental spectra, with all other FTS settings being the same). In practice, this means that it is necessary to trade off between instrumental resolution and noise level to optimize the signal-to-noise ratio of a given spectrum[21]. Although this is easily realized with Fourier-transform spectroscopy, this property is not available, or only for a very limited range, for VUV laser sources based upon four-wave mixing for which the instrumental linewidth is fixed, as given by the pumping laser, and not directly linked to the generated VUV flux.

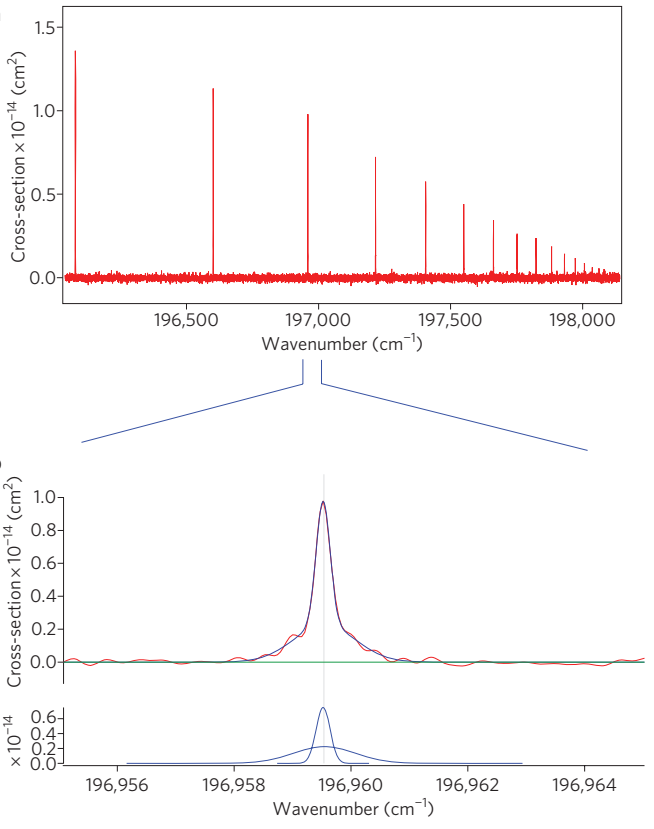

Figure 3 | Helium photoabsorption cross-section using the free expansion jet set-up. a, Absolute absorption cross-section of the Rydberg series of helium converging towards the $1s^{-1}$ ($^2S_{1/2}$) ionization threshold ($n = 8$–20). **b**, Enlarged view of the $1s \rightarrow 9p$ transition. The cross-section is fitted using two Gaussian curves with two different FWHM corresponding respectively to the cold ($0.29\ cm^{-1}$) and room-temperature ($1.24\ cm^{-1}$) contributions. The room-temperature contribution has been set to $1.24\ cm^{-1}$ (convolution of the theoretical Doppler width and instrument linewidth). The cold-contribution linewidth is close to the instrument resolution for $p = 14$, $0.25\ cm^{-1}$, its corresponding Doppler temperature being below 10 K. The absolute cross-section is calibrated on the cold part considering theoretical oscillator strength calculations from the literature[27].

Table 2 | Level-to-noise ratio measured experimentally throughout the FTS range from 55,000 to 200,000 cm^{-1}.

Position of the undulator peak (cm^{-1})	55,000	65,000	75,000	85,000	95,000	110,000	120,000	130,000	145,000	165,000	180,000	200,000
Level-to-noise ratio	970	565	465	245	175	230	225	205	250	215	230	165

The level is the maximum of the undulator spectrum; the noise is the corresponding r.m.s. amplitude. Each column corresponds to different central undulator energies. Results are normalized for 60 min of integration time and a spectral linewidth $\delta\sigma = 0.25$ cm^{-1}. These figures take into account all experimental parameters, in particular the source emission and beamline transmission. The experimental noise was estimated to be three times the photon noise limit.

To characterize the FTS instrument (including the source), Table 2 presents experimental noise data measured with various FTS and source settings at the undulator peak. The noise data are referred to the maximum source spectral level, as this scales the absorption signal, and the result is presented in terms of level-to-noise ratio. The FTS resolution is set to 0.25 cm^{-1}, and the noise is reduced by co-adding several spectra, corresponding to a total acquisition time of 60 min.

As well as the wavenumber scale accuracy aspects and the ultimate resolving power, level-to-noise ratio is an overall figure of merit, with which it is interesting to compare Fourier-transform spectroscopy with other broadband VUV absorption spectroscopy techniques. In particular, we have been able to perform a direct comparison with experimental data recorded using a high-resolution state-of-the-art grating monochromator[7] from the third-generation synchrotron radiation undulator-based beamline (DESIRS)[15]. To achieve the same given level-to-noise ratio and moderate resolution ($\delta\sigma = 1.3$ cm^{-1}) over a spectral range with a width of 6,000 cm^{-1}, which is the typical bandwidth covered by the FTS around 100,000 cm^{-1}, the recording time with the monochromator is ~30 times longer than with the FTS. This could appear paradoxical, as the wavefront-division interferometer does not show an aperture advantage and is at best limited by photon noise, like the grating spectrometer. The main difference lies in the dead time (acquisition, electronics and mechanical) between recorded points, which cannot be less than 0.5 s on the DESIRS beamline, as in any existing scanning monochromator. We should also mention the loss of flux on the monochromatic branch due to the two extra reflections onto the pre- and post-focusing mirrors of the monochromator. This spectacular gain is particularly interesting when the spectroscopic information is very dense and spread out through a large spectral domain, as in the case of dense predissociative Rydberg states series[22] and super-excited states[23] in the region of the different valence shell ionization limits. Therefore, even in the case of 'moderate' resolution, the FTS can be a unique tool. For instance, spectrum with a coarse 6 cm^{-1} resolution and with a level-to-noise ratio of ~60 can be recorded over the 7% bandwidth in 10 s, which is orders of magnitude faster than with existing scanning grating-based monochromators. This feature may give access to real-time spectroscopic probing of slow chemical reactions, such as aerosols growing in smog chambers or nanoparticles in solution.

We believe that this new Fourier-transform-based instrument, because of its unprecedented resolving power, absolute line position accuracy, very broad allowed domain and its effective very high data acquisition efficiency, will soon lead to unique results in gas-phase absorption spectroscopy over the whole VUV range. Projects using the FTS are ongoing in relation to astrophysics in the fields of cosmology[24], interstellar media[25] and planetary atmosphere[26], for which there is a crucial need for accurate high-resolution laboratory databases with which to interpret airborne-spectrometer and telescope data. Breakthroughs are also expected in the study of the terrestrial atmosphere and combustion processes, including the spectroscopy of radicals, as well as in plasma physics. In principle, the FTS could also be applied to emission spectroscopy for the study of highly ionized atomic states, provided that high-luminance VUV emission sources are available.

Received 26 July 2010; accepted 6 December 2010;
published online 23 January 2011

References

1. Thorne, A. High resolution Fourier transform spectrometry in the visible and ultraviolet regions. *J. Anal. At. Spectrom.* **13,** 407–411 (1998).
2. Eikema, K. S. E. & Ubachs, W. *Handbook of High Resolution Spectroscopy. Precision Laser Spectroscopy in the Extreme Ultraviolet* (eds Quack, M. & Merkt, F.) (John Wiley & Sons, 2010).
3. Rupper, P. & Merkt, F. Intense narrow-bandwidth extreme ultraviolet laser system tunable up to 20 eV. *Rev. Sci. Instrum.* **75,** 613–622 (2004).
4. Ubachs, W., Eikema, K. S. E., Hogervorst, W. & Cacciani, P. C. Narrow-band tunable extreme-ultraviolet laser source for lifetime measurements and precision spectroscopy. *J. Opt. Soc. Am. B* **14,** 2469–2476 (1997).
5. Paul, Th. A. & Merkt, F. High-resolution spectroscopy of xenon using a tunable Fourier-transform-limited all-solid-state vacuum-ultraviolet laser system. *J. Phys. B.* **38,** 4145–4154 (2005).
6. Trickl, T., Kung, A. H. & Lee, Y. T. Krypton atom and testing the limits of extreme-ultraviolet tunable-laser spectroscopy. *Phys. Rev. A* **75,** 022501 (2007).
7. Nahon, L. *et al.* Very high spectral resolution obtained with SU5: a vacuum ultraviolet undulator-based beamline at Super-ACO. *Rev. Sci. Instrum.* **72,** 1320–1329 (2001).
8. Reichardt, G. *et al.* A 10 m-normal incidence monochromator at the quasi-periodic undulator U125-2 at BESSY II. *Nucl. Instrum. Methods A* **467,** 462–465 (2001).
9. Ito, K. *et al.* High-resolution VUV spectroscopic facility at the Photon Factory. *Appl. Opt.* **25,** 837–847 (1986).
10. Pickering, J. C. High resolution Fourier transform spectroscopy with the Imperial College (IC) UV-FT spectrometer, and its applications to astrophysics and atmospheric physics: a review. *Vib. Spectrosc.* **29,** 27–43 (2002).
11. Strong, J. & Vanasse, G. A. Lamellar grating far-infrared interferometer. *J. Opt. Soc. Am.* **50,** 113–118 (1960).
12. Howells, M. R. *et al.* Toward a soft X-ray Fourier-transform spectrometer. *Nucl. Instrum. Methods Phys. Res. A* **347,** 182–191 (1994).
13. Polack, F., Joyeux, D., Svatoš, J. & Phalippou, D. Applications of wavefront division interferometers in soft X rays. *Rev. Sci. Instrum.* **66,** 2180–2183 (1995).
14. de Oliveira, N. *et al.* A Fourier transform spectrometer without a beam splitter for the vacuum ultraviolet range: from the optical design to the first UV spectrum. *Rev. Sci. Instrum.* **80,** 43101 (2009).
15. DESIRS beamline website, www.synchrotron-soleil.fr/portal/page/portal/Recherche/LignesLumiere/DESIRS.
16. Marcouille, O. *et al.* Design, construction and magnetic measurements of the HU640 (OPHELIE2) undulator dedicated to the DESIRS VUV beamline at SOLEIL. *AIP Conf. Proc.* **879,** 311–314 (2007).
17. Forman, M. L., Steel, W. H. & Vanasse, G. A. Correction of asymmetric interferograms obtained in Fourier spectroscopy, *J. Opt. Soc. Am.* **56,** 59–61 (1966).
18. Maeda, K., Ueda, K. & Ito, K. High-resolution measurement for photoabsorption cross sections in the autoionization regions of Ar, Kr and Xe. *J. Phys. B* **26,** 1541–1555 (1993).
19. Sommavilla, M., Hollenstein, U., Greetham, G. M. & Merkt, F. High-resolution laser absorption spectroscopy in the extreme ultraviolet *J. Phys. B* **35,** 3901–3921 (2002).
20. Brault, J. W. High precision Fourier transform spectrometry: the critical role of phase corrections. *Mikrochim. Acta* **III,** 215–227 (1987).
21. Davis, S. P., Abrams, M. C. & Brault, J. W. *Fourier Transform Spectrometry* (Academic Press, 2001).
22. Stark, G. *et al.* Oscillator strength and linewidth measurements of dipole-allowed transitions in $^{14}N_2$ between 93.5 and 99.5 nm. *J. Chem. Phys.* **123,** 214303 (2005).
23. Glass-Maujean, M. *et al.* H_2 superexcited states: experimental and theoretical characterization of their competing decay-channel fluorescence, dissociation, and ionization. *Phys. Rev. Lett.* **104,** 183002 (2010).

24. Reinhold, E. *et al.* Indication of a cosmological variation of the proton-electron mass ratio based on laboratory measurement and reanalysis of H_2 spectra. *Phys. Rev. Lett.* **96,** 151101 (2006).
25. Eidelsberg, M. *et al.* Oscillator strengths and predissociation rates for Rydberg transitions in $^{12}C^{16}O$, $^{13}C^{16}O$, and $^{13}C^{18}O$ involving the E $^1\Pi$, B $^1\Sigma^+$, and W $^1\Pi$ state. *Astrophys. J.* **647,** 1543–1548 (2006).
26. Hansen, C. J. *et al.* Enceladus' water vapor plume. *Science* **311,** 1422–1425 (2006).
27. Kono, A. & Hattori, S. Accurate oscillator strengths for neutral helium. *Phys. Rev. A* **29,** 2981–2988 (1984).

Acknowledgements

This work was supported by the ANR (Agence Nationale de la Recherche; grant 05-BLAN-0364). The authors acknowledge the invaluable skill of the Optical Surface and Component group from the Laboratoire Charles Fabry for fabrication of the optical parts and metrology. Warm thanks go to B. Pilette and J.-F. Gil for their contribution to the conception and mounting of the sample chamber, as well as M. Vervloet (Synchrotron SOLEIL) and K. Ito (Photon Factory, Tsukuba, Japan) for fruitful discussions on spectroscopic issues. The authors are also grateful to the general technical staff of the synchrotron SOLEIL facility.

Author contributions

N.d.O., D.J., D.P. and J.C.R. designed and built the Fourier transform instrument. N.d.O., D.J. and L.N. designed the whole absorption facility set-up, including the beamline coupling and the sample chamber. N.d.O., M.R. and D.J. performed the experiments and analysed the data. L.N. supervised the scientific coherence of the Fourier transform project. N.d.O., D.J., L.N. wrote the manuscript.

Additional information

The authors declare no competing financial interests. Reprints and permission information is available online at http://npg.nature.com/reprintsandpermissions/. Correspondence and requests for materials should be addressed to N.d.O.